Biodegradation **12:** 401–410, 2001.

Uranyl precipitation by biomass from an enhanced biological phosphorus removal reactor

Neil Renninger[1], Katherine D. McMahon[2], Roger Knopp[3], Heino Nitsche[3,4], Douglas S. Clark[1] & Jay D. Keasling[1,*]

[1]*University of California at Berkeley, Department of Chemical Engineering, Berkeley, CA 94720-1462, USA;* [2]*University of California at Berkeley, Department of Civil and Environmental Engineering, Berkeley, CA 94720-1710, USA;* [3]*Lawrence Berkeley National Laboratory, The Glenn T. Seaborg Center, Berkeley, CA 94720, USA;* [4]*University of California at Berkeley, Department of Chemistry, Berkeley, CA 94720-1460, USA (* author for correspondence)*

Accepted 8 November 2001

Key words: enhanced biological phosphorus removal, heavy metal removal, polyphosphate

Abstract

Heavy metal and radionuclide contamination presents a significant environmental problem worldwide. Precipitation of heavy metals on membranes of cells that secrete phosphate has been shown to be an effective method of reducing the volume of these wastes, thus reducing the cost of disposal. A consortium of organisms, some of which secrete large quantities of phosphate, was enriched in a laboratory-scale sequencing batch reactor performing Enhanced Biological Phosphorus Removal, a treatment process widely used for removing phosphorus. Organisms collected after the aerobic phase of this process secreted phosphate and precipitated greater than 98% of the uranyl from a 1.5 mM uranyl nitrate solution when supplemented with an organic acid as a carbon source under anaerobic conditions. Transmission electron microscopy, energy dispersive x-ray spectroscopy, and fluorescence spectroscopy were used to identify the precipitate as membrane-associated uranyl phosphate, UO_2HPO_4.

Abbreviations: EBPR – enhanced biological phosphorus removal, EDXS – energy dispersive X-ray spectroscopy

Introduction

Recently, interest in biological methods for heavy metal and radionuclide removal from waste streams has increased significantly due to their advantages over traditional wastewater treatment processes (chemical precipitation, electrochemical methods, ion exchange or filtration), which become prohibitively expensive with metal concentrations on the order of 1 to 100 mg l^{-1} (Volesky 1990). Much of the work in this area has focused on the isolation of specific bacteria (Wang et al. 1997; Alonso et al. 2000; Llanos et al. 2000; Nies 2000; Sharma et al. 2000; Xiang et al. 2000) and algae (Mallick et al. 1996; Wang et al. 1998; Travieso et al. 1999) having intrinsic metal tolerance and metal-binding capabilities, as well as the engineering of organisms towards the development of metal binding capabilities (Chen & Wilson 1997; Bang et al. 2000; Valls et al. 2000; Wang et al. 2000).

Macaskie and Dean (1982) isolated a cadmium resistant strain of *Citrobacter* which bound cadmium, uranyl, americium, and other heavy metals and actinides through the use of a membrane-bound acid phosphatase (Macaskie et al. 1987, 1992; Macaskie 1990). Using glycerol-2-phosphate as a phosphate source, the organism cleaved phosphate from the source at the inner membrane, leaving it to bind with metals that had been complexed by citrate in solution. Complexation was required, since the acid phosphatase was sensitive to the presence of free metal in solution (Yong & Macaskie 1995). The insoluble metal-phosphates precipitated on the surface of the cells.

Previous work has shown that engineered *E. coli* harboring multiple copies of the genes for polyphos-

phate kinase and exopolyphosphatase, enzymes responsible for the synthesis and degradation of polyphosphate, was able to tolerate increased concentrations of heavy metals such as cadmium (Keasling & Hupf 1996). This work suggested that the ability to turn over polyphosphate reserves was more important to metal resistance than simply the ability to accumulate polyphosphate.

We identified biomass derived from Enhanced Biological Phosphorus Removal (EBPR) reactors as a possible source of metal-accumulating bioadsorbant. EBPR is a wastewater treatment process used directly for the efficient removal of high phosphorus loads in wastewater, or indirectly to increase beneficial settling characteristics of the biomass sludge (Van Loosdrecht et al. 1997).

During EBPR, influent wastewater, generally high in both phosphorus and fatty acid content, is pumped into an anaerobic reactor containing activated sludge. Intracellular phosphate stores (polyphosphate) are depleted and phosphate is secreted from the cell as fatty acids are accumulated and stored as poly-hydroxyalkanoates (PHAs). The wastewater and sludge are then pumped into an aerobic tank in which biomass increases, PHAs are depleted, and phosphate is accumulated as polyphosphate, reducing phosphate concentrations in the wastewater to 1–2 mg l^{-1}. Biomass sludge is then settled from the mix, and a portion of the sludge is recycled to the first reactor for anaerobic contacting with fresh wastewater.

As noted previously, phosphate secretion has been an efficacious cellular process for the biosorption of heavy metals and actinides. In the present work, we investigate the use of EBPR sludge as a possible metal and actinide biosorbant, using biomass from an enriched sequencing batch reactor operating in our laboratory.

Materials and methods

Establishment of EBPR reactor

A 1-l sequencing batch reactor, inoculated with a seed of mixed liquor from the City of San Francisco, Southeast Water Pollution Control Plant in 1996 was operated on a 6-h cycle (30-min draw and fill, 120-min anaerobic phase, 180-min aerobic phase, and 30-min settling). An automated pumping system maintained a 12-h hydraulic residence time and a 4-d sludge age. A mineral salts-based nutrient feed (Wentzel et al. 1988) contained various amounts of inorganic phosphate to control the influent chemical oxygen demand to phosphorus (COD/P) ratio. During the time when samples were taken for the current study, COD/P ratios were approximately 20 g COD/g P, producing a sludge P-content of around 0.15 g P/(g volatile suspended solids) and a biomass content of approximately 0.7 mg DCW per l. A separate carbon feed solution containing acetate and casamino acids gave a fixed COD loading of 115 mg COD/L/cycle. The reactor was routinely sampled for soluble P, suspended solids, and total P using standard methods, to verify steady state performance.

Uranyl binding experiments

100-ml samples of biomass from the end of the aerobic cycle were removed from the reactor, centrifuged at 10,000 g for 10 min, washed with an equal volume of 50 mM NaCl solution, centrifuged again, and resuspended in an equal volume of medium containing solely 1.5 mM UO_2NO_3 and 10 mM sodium acetate, pH 7.0 in capped bottles. The headspaces of each of the bottles were flushed briefly with nitrogen. These bottles were placed in a room temperature shaker at 200 rpm. 5 ml samples were removed via a syringe, and centrifuged. The pellet was saved at -70 °C for polyphosphate analysis while the supernatant was saved at -20 °C for analysis for phosphate and uranyl.

1-ml samples were also taken by syringe and passed through a 0.22-μm ore diameter filter to study the residual uranyl in the filtrate. During the course of the experiments, the pH remained at roughly 7.0 as the acetate buffers the system.

Uranyl assay

Uranyl concentration was assayed using the Arsenazo III reagent (Fritz & Bradford 1958). A sample of 20 μl was added to 50 μl of Arsenazo reagent (60 mg ml^{-1}) and 450 μl of 0.5 M HCl. The absorbance was recorded at a wavelength 652 nm on a Beckman DU640 spectrophotometer. Concentrations were calculated by comparing to a standard curve. Uranyl assays were performed in triplicate.

Polyphosphate assay

Polyphosphate was measured using one of two assays. In the absence of heavy metals, polyphosphate was measured by binding polyphosphate to Glassmilk^{TM} (silica glass – Q-Biogene, Carlsbad, CA) (Ault-Riche

et al. 1998). In the presence of heavy metals, this assay is ineffective, due to the interference of uranyl with the binding of polyphosphate to Glassmilk. In this case, polyphosphates were extracted, hydrolyzed with 0.1 M HCl at 95 °C for 1 h, and analyzed for phosphate (Sharfstein et al. 1996). Polyphosphate assays were performed in triplicate.

Inorganic phosphate concentration assay

Phosphate concentration was measured with the Calcium/Phosphorus Measurement Kit (Sigma). A 20-μl sample was added to 500 μl of aluminum molybdate reagent. The absorbance was measured at a wavelength of 340 nm and compared to a set of standards. Phosphate assays were performed in triplicate.

TEM/EDXS

One ml samples were fixed in a 2% glutaraldehyde solution at 4 °C for 12 h. Samples were then dehydrated with a series of 5-min acetone:water washes of increasing acetone concentration, up to a pure acetone wash. Samples were then infiltrated with an epoxy resin through a series of resin:acetone infiltrations of increasing resin concentration, and left to harden overnight. Samples were sectioned using an MT-6000 microtome, placed on 100 mesh carbon-coated copper grids, and analyzed using a JEOL transmission electron microscope.

Energy dispersive X-ray spectroscopy was performed using a JEOL 200CX microscope with two Kevex EDX detectors coupled to a computer running Emispec analytical software. Elemental analysis was performed through the comparison of uranium m-peaks with phosphorus *k*-peaks.

Time resolved laser induced fluorescence spectroscopy

For the excitation of U(VI) a pulsed Nd-YAG laser (Spectra Physics, GCR-3) operating at a wavelength of 355 nm was used. The wavelength of 355 nm is achieved by third harmonic generation of the 1064 nm emission of the Nd-YAG laser with two KD*P crystals. The laser was operated at a pulse energy of about 1 mJ. Laser energy was monitored by a calibrated energy meter (Newport, 1812C) placed in the reflex of the laser beam from a quartz plate placed in the beam with a 45° angle to the beam axis. The laser beam then passes through a rectangular quartz cuvette with 3 ml volume containing the samples. The fluorescence emission, perpendicular to the laser beam axis, is focused by a lens system onto the entrance slit of a spectrograph (Acton Research, Spectra Pro 500i). The spectrograph provides three gratings. For our experiments, a grating with 300 lines per mm and a spectral resolution of 0.2 nm was used. The fluorescence emission was detected by an intensified, gated CCD-camera system (Princeton Instruments, PI-Max). A combined camera controller, pulser and timing generator (Princeton Instruments, ST-133) can set a variable time delay and time gate, respectively to the laser pulse for the measurements. A delay time of 2 μs after the lamp trigger signal of the laser was found to be optimal to discriminate light scattering. The gate width was set to 1 μs. 100 spectra were accumulated for every measurement. All functions of the spectrograph, controller, pulser, timing generator and CCD-camera and the data collection were controlled by a personal computer using the program Winspec 2.4 (Princeton Instruments).

Biomass samples were centrifuged, washed in 50 mM potassium nitrate, centrifuged, and resuspended in 50 mM potassium nitrate before analysis to remove any remaining uranyl from solution. The final pH after wash and resuspension is roughly 4.5. Therefore, all comparisons are made to solutions also at pH 4.5.

Results and discussion

The EBPR reactor provided a biomass sludge that was highly enriched in phosphorus, resulting in a 20% w/w phosphorus content. The microbial community structure in the sequencing batch reactor was similar to that of other EBPR sludges maintained under similar conditions (Hesselmann et al. 1999; Crocetti et al. 2000). Clone libraries consisting of 16S rDNA genes PCR-amplified from DNA extracted from the sludge used in the current study (K. D. McMahon and J. D. Keasling, unpublished results) contained a sequence type that was 99% identical to the "R6" clone identified by Hesselmann and coworkers (Hesselmann et al. 1999; Crocetti et al. 2000). This *Rhodocyclus*-like organism constituted approximately 75% of total bacteria in the sludge, as determined by fluorescent in situ hybridization (K. D. McMahon and J. D. Keasling, unpublished results). These results suggest that these organisms were responsible for polyP accumulation in this EBPR sludge.

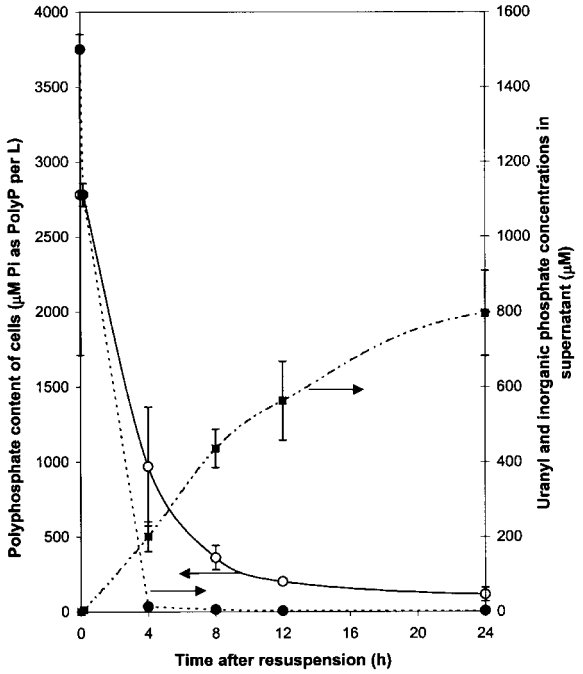

Figure 1. Polyphosphate degradation, inorganic phosphate release, and uranyl removal by the EBPR consortium. 200 ml of 0.7 g DCW/l EBPR culture was harvested after the aerobic phase and resuspended in 10 mM sodium acetate, 1.5 mM uranyl nitrate. Uranyl removal followed polyphosphate degradation, resulting in over 99% removal of initial uranyl. Filled circles (●), uranyl; open circles (○), polyphosphate content of cells; filled squares (■), inorganic phosphate in medium. Error bars indicate the standard deviation of triplicate samples and are shown only when larger than the symbols.

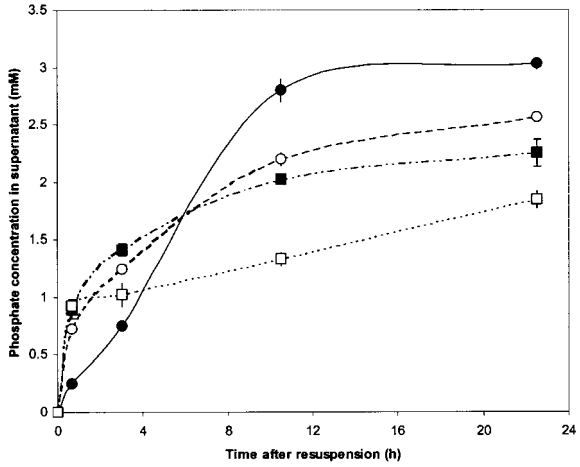

Figure 2. Phosphate release with varying initial acetate concentrations in the absence of metal. The EBPR culture was harvested after the aerobic phase and resuspended in varying levels of acetate. Increasing levels of acetate resulted in increased cumulative phosphate release with decreased initial rates. Filled circles (●), 1 M acetate; open circles (○), 100 mM acetate; filled squares (■), 10 mM acetate; open squares (□), 1 mM acetate.

EBPR biomass was centrifuged and resuspended in an equal volume of 10 mM sodium acetate, 1.5 mM uranyl nitrate solution in anaerobic bottles as described above. Phosphate release and concomitant uranyl removal from the supernatant was observed (Figure 1). Filtrate of samples collected simultaneously to centrifuged samples provided uranyl and phosphate concentrations that agreed to within 2% (data not shown), suggesting that precipitation occurred at the point of phosphate release. If precipitation had occurred in the bulk solution, the precipitate would be much finer, allowing most of it to pass through the filter. An equal mix of 3 mM potassium phosphate with 2 mM uranyl nitrate resulted in a fine precipitate, 80% of which passed through a 0.2 micron filter. This percentage does not change with time.

Greater than 99% of the metal was removed over a 4 hour period. Phosphate did not begin to appear in the supernatant until the uranyl concentration reached a minimum. Residual uranyl probably remained in the supernatant due to complexation with acetate or cellular products. Results of typical experiments are shown. While the trajectories of phosphate release, polyphosphate degradation, and uranyl removal were always quite similar, the magnitude of the phosphorus content of the sludge changed slightly in the reactor from day to day, making direct comparison of different experiments impractical.

Cells were ultimately loaded with over 50% of their dry cell weight in uranium. This binding capacity is significantly higher than the approximately 30%w/w loadings attainable through the use of commercial ion exchange resins, such as Dowex 21 K, thus reducing the ultimate volume of waste produced.

Variation in the initial acetate concentration provided varying initial rates of phosphate release as well as final uranyl concentrations. Generally, lower acetate concentrations led to higher initial rates of phosphate release, but lower amounts of cumulative phosphate secreted (Figure 2) when resuspended in the absence of uranyl. Results are shown from a typical experiment. Trends seen in this experiment were observed in similar experiments. In the presence of uranyl, uranyl removal trajectories were very similar to phosphate secretion trajectories in the absence of uranyl (Figure 3). The uranyl concentration in the supernatant after 24 hours was 6.0, 2.7, 30 and 67 μM for initial actetate concentrations of 1, 10, 100, and 1000 mM, respectively.

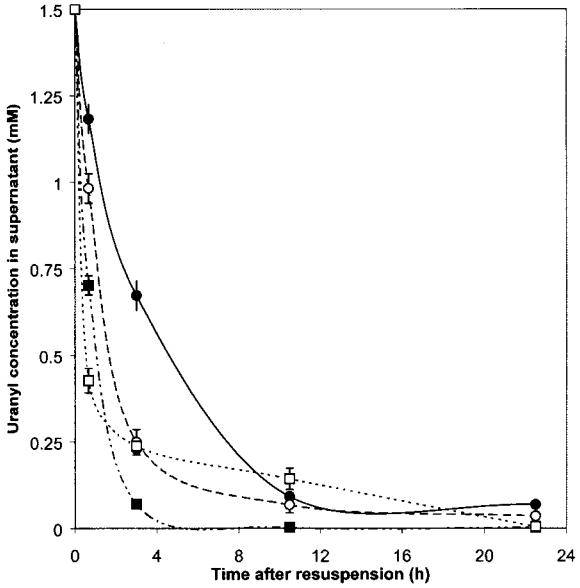

Figure 3. Uranyl removal with varying initial acetate concentrations. EBPR culture was harvested after the aerobic phase and resuspended in 1.5 mM uranyl nitrate with varying levels of acetate (Ac) as shown. Decreasing acetate levels generally decreased the final concentration of uranyl remaining in solution. Trajectories were very similar to phosphate secretion trajectories. Filled circles (●), 1 M acetate; open circles (○), 100 mM acetate; filled squares (■), 10 mM acetate; open squares (□), 1 mM acetate.

The differences in phosphate secretion trajectories are somewhat surprising, but initially may have more to do with equalization of osmolarities than polyphosphate metabolism. That is, the initial release of phosphate may be used more to overcome osmotic stress than it is used to recharge the transmembrane proton gradient for acetate assimilation.

The increase in cumulative phosphate release with acetate concentration is not surprising, because the phosphate energetically drives the uptake of fatty acids (Van Veen et al. 1994). It has been proposed that phosphate from polyphosphate is transferred to ATP via polyphosphate:AMP phosphotransferase and adenylate kinase. This ATP is then used to drive the uptake and conversion of acetate to acetyl-CoA, while also freeing phosphate to be released from the cell. The freed phosphate, released partially protonated, helps to increase the transmembrane proton gradient, aiding the uptake of the negatively charged fatty acid and helping the generation of ATP. The result is generally a consistent molar ratio of phosphate released to carbon moles assimilated, a molar ratio that ranges from 0.25 to 0.75 for acetate (Smolders et al. 1994). The ratio observed in this work for a carbon loading of 1 mM acetate (likely carbon limited after 2 h) approached 0.75. Therefore, greater phosphate releases for higher concentrations of acetate is to be expected given the energetics of fatty acid accumulation.

Energy-dispersive X-ray spectroscopy was used to identify the location and nature of the uranyl precipitate (Figure 4). Uranyl phosphate appeared as intracellular bodies, forming spheres around unidentified bodies as well as at the membrane of cells, and as large extracellular crystals, up to two microns in length, associated with the cell membranes. It is unknown whether the preparation of samples for TEM caused cells to lyse, releasing the large intracellular crystals, or if these bodies existed prior to sample preparation. However, noting the size of the extracellular bodies, it can be assumed that these crystals never could have existed intracellularly, and thus must have formed as extracellular crystals. It is likely that the unknown bodies, shown in Figure 5a, are granules of PHAs, mainly polyhydroxybutyrate. This amorphous body inside the cell may initially chelate some of the uranyl that enters the cell. Such chelated uranyl could then bind with phosphate released from the degradation of polyphosphate, forming the electron dense precipitate observed inside the cell.

A comparison of micrographs of a culture two hours after resuspension in uranyl and acetate with those 12 hours after resuspension (Figure 5) suggests that these crystals begin their formation at the cell membrane, grow to a very large size (crystals up to 2 microns long were observed), and then may fall off of the cells or separate from the cells during preparation. Small crystals must be cell associated, because they would have passed through a 0.22 μm filter, thus increasing the concentration of uranyl in the filtrate over that of the supernatant samples. EDXS identified this compound to be 49.1% uranium and 50.9% phosphorus, suggesting UO_2HPO_4.

Uranium in the oxidation state U(VI) dissolved in aqueous solutions forms the uranyl cation (UO_2^{2+}). The uranyl cation can be excited with ultraviolet light and the relaxation of excited electronic levels of uranyl results in fluorescent light emission. A time- and wavelength-resolved fluorescence spectrum of uranyl is measured by time resolved laser induced fluorescence spectroscopy. The lifetime of the fluorescence, the wavelength of maximum fluorescence intensity, and the width of fluorescence peaks depend on the chemical environment of the uranyl cation. Therefore, the exact chemical speciation of uranyl complexes can be performed by time-resolved laser-induced fluores-

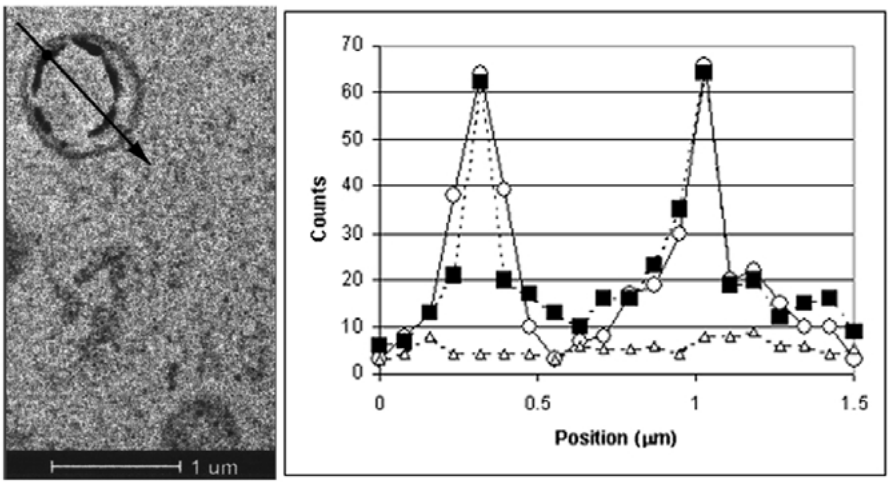

Figure 4. Energy dispersive X-ray spectroscopy of a sample cell. The graph shows results of a line scan through a cell as shown by the large arrow in the micrograph. Uranium counts are shown by circles, phosphorus counts are shown by squares, and background counts are shown by triangles. The dotted vertical line represents the position of the black dot (highlighted by the small arrow) near the beginning of the large arrow. These results show the presence of uranyl and phosphorus at the dark regions inside the cell. Elemental analysis showed these two elements to be in a 1:1 stoichiometry.

cence spectroscopy (Moulin et al. 1994; Bernhard et al. 1996). Furthermore, the presence of fluorescent species removes any doubt that the uranium may have been reduced to uranyl(IV) as has been seen in other biological cases (Lovley 1995; Tucker et al. 1998; Fredrickson et al. 2000), since it is the excitation of the axial oxygen bonds that results in the fluorescence.

Changes in the inner sphere complexation of the uranyl cation can be easily monitored by changes in the fluorescence spectrum (Figure 6). At pH 1, the free uranyl cation is the only species present (spectrum I). By increasing the pH from 1 to 4.5 the uranyl forms various hydrolysis products (UO_2OH^+, $(UO_2)_2(OH)_2^{2+}$ and $(UO_2)_3(OH)_5^+$ are dominant at pH 4.5 (Kato et al. 1994; Moulin et al. 1995; Kitamura et al. 1998) by complexation with hydroxyl anions (OH^-). The corresponding spectrum (II) differs significantly from that of the free uranyl cation. The different fluorescence properties and the mixture of various species leads to emission peaks that are shifted in wavelength (Table 1) and are not clearly resolved. By adding a suspension of EBPR-culture (pH 4.5) to the uranyl solution at pH 4.5, the fluorescence spectrum changes drastically (spectrum III). The peak shift (Table 1) and the shape of the resulting spectrum correspond well to that of an uranyl-polyphosphate complex at pH 4.5 (spectrum IV). This polyphosphate complex is used for comparison rather than monophosphate complexes, because at pH 4.5 uranyl monophosphates tend to precipitate. For uranyl phosphates, changes in spectra can be seen with changes in the atom directly bound to the phosphate. For example, uranyl-AMP gives a different spectrum than does uranyl-ATP which gives the same spectrum as inorganic uranyl phosphate. Peak maxima of uranyl monophosphate complexes stable at pH 3 show no significant deviation from those of the polyphosphate complex at pH 4.5 (Table 1). The spectrum of an uranyl-ATP complex (Table 1) with a binding of U(VI) to a terminal phosphate group is also very similar to that of the uranyl-polyphosphate, reflecting the same chemical environment of the uranyl. A different spectrum is found for an uranyl-AMP complex (spectrum V). AMP, with a phosphate group directly bound to an organic group in the molecule, resembles very well the structure of teichoic acids, which are considered major sites for the sorption of U(VI) on the cell surface. From the similarity of the spectrum of the uranyl-EBPR culture with that of the uranyl polyphosphate complex and the differences with the spectrum of the uranyl-AMP complex, it can be concluded that the uranyl is precipitated by phosphate released by the EBPR culture and that sorption of uranyl to the surface of the bacteria (without precipitation by phosphate) is not a major contribution. Furthermore, the fact that the peaks resulting from precipitation by the EBPR culture are slightly broader than those from a pure phosphate precipitate further suggests another influence, likely that of cell attachment.

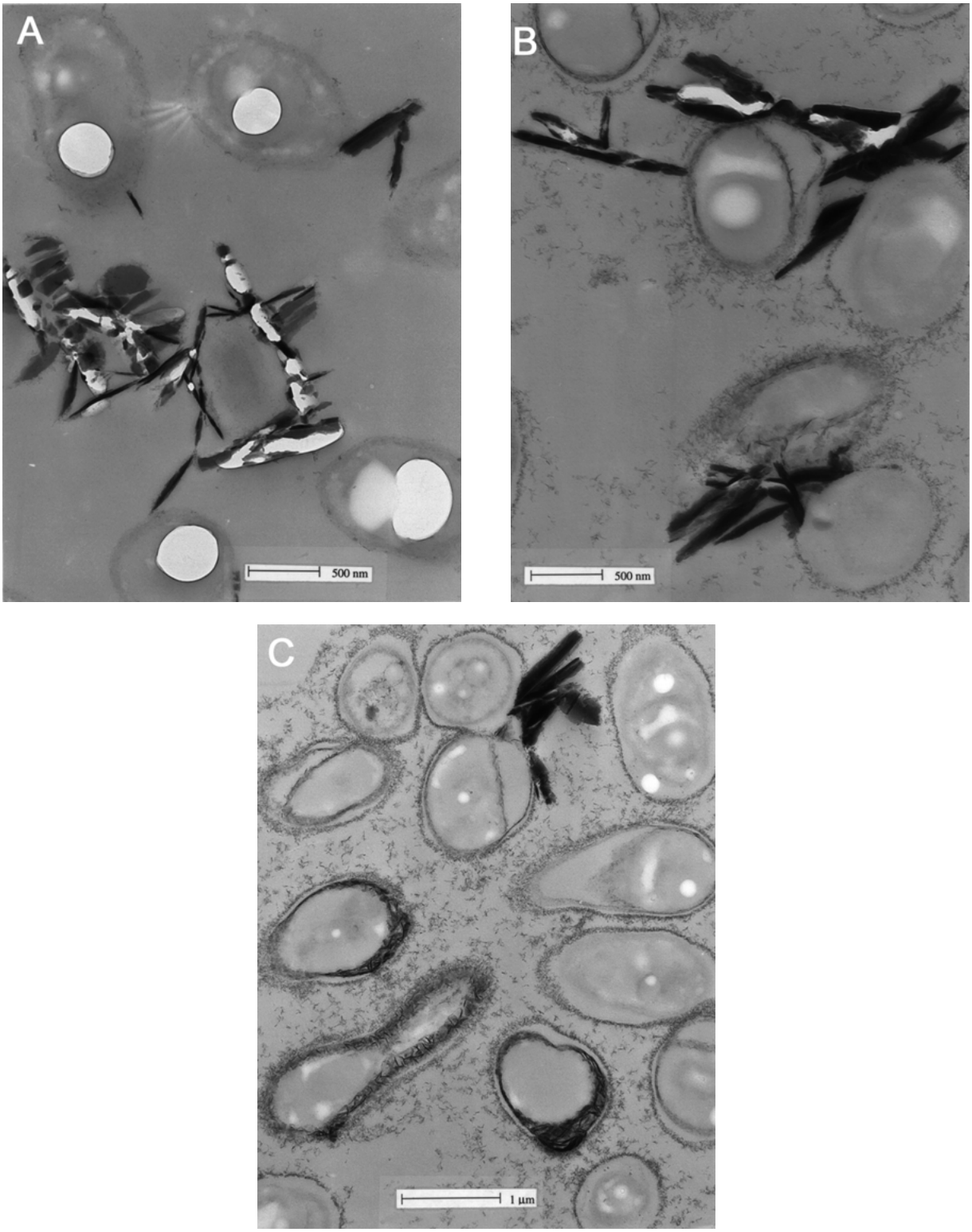

Figure 5. Transmission electron micrograph of EBPR samples 2 h (A) and 12 h (B, C) after resuspension in uranyl nitrate. Suspected PHB globules surrounded by uranyl nitrate are seen in (A). Note the large extracellular crystals of uranyl phosphate in each sample, as well as the small crystals making up the membrane in the samples incubated for a longer period of time.

Table 1.

Species	Main fluorescence wavelengths (nm)				Source
UO_2^{2+} at pH 1	487, 488	510, 509	533, 534	560, 560	(Kato et al. 1994; Moulin et al. 1995; Kitamura et al. 1998)
UO_2^{2+} at pH 1	488	510	534	560	This work
UO_2^{2+} hydrolysis at pH 4.98	500*	516	533	555*	Kato et al. (1994)
UO_2^{2+} hydrolysis at pH 4.5	500*	515	534	558*	This work
UO_2^{2+} EBPR culture, pH 4.5	495	517	540	567	This work
UO_2^{2+} polyphosphate, pH 4.5	494	516	540	566	This work
$UO_2H_2PO_4^+/UO_2HPO_4$, pH 3	494	517	541	565	Bernhard et al. (1996)
UO_2^{2+} ATP pH 4.5	495	517	540	566	This work
UO_2^{2+} AMP pH 4.5	497	519	542*	569*	This work

* Fluorescence peaks not clearly resolved, estimated maximum.

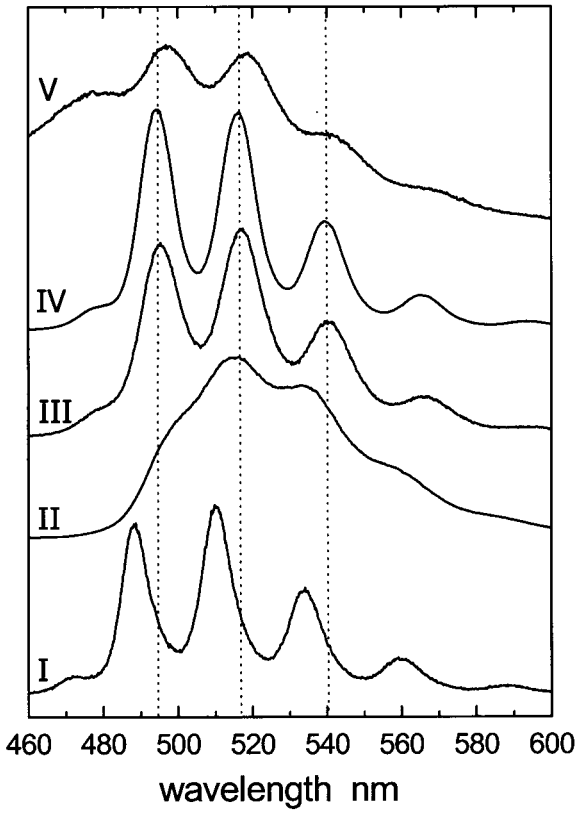

Figure 6. Time resolved laser induced fluorescence spectra of the uranyl cation (UO_2^{2+}): (I) Free uranyl cation at pH 1. (II) Uranyl-hydolysis species at pH 4.5: UO_2OH^+, $(UO_2)_2(OH)_2^{2+}$ and $(UO)2)_3(OH)_5^+$ dominant at pH 4.5 (Kato et al. 1994; Moulin et al. 1995; Kitamura et al. 1998) (III) Uranyl with EBPR bacteria at pH 4.5. (IV) Uranyl-polyphosphate complex at pH 4.5.(V) Uranyl-adenosinemonophosphate complex at pH 4.5.

Conclusions

This work shows the utility of biomass generated from an EBPR process in the sequestration of aqueous actinides. Through fluorescence spectroscopy, it was shown that a model actinide, uranyl ion, initially sorbs to the biomass as a hydroxide. Upon secretion of phosphate under anaerobic conditions, sorbed uranyl is precipitated as uranyl phosphate. Precipitation continues as phosphate is continuously secreted from the cell, forming large crystals of uranyl phosphate, which are attached to the cell as identified by TEM and EDXS. The entire process is fairly quick, as 65% and 85% of the cellular polyphosphate is degraded within 4 and 8 hours, respectively.

The polyphosphate-enriched biomass obtained through the EBPR process was able to accumulate large amounts of uranyl, resulting in a uranyl loading of 600 mg/g DCW. This is extremely high, especially when compared to current ion exchange resins, which can be loaded up to 30% w/w. Unlike resins, the biomass cannot be reused. It can, however, be obtained very economically from wastewater treatment plants in many parts of the world, which send much of the biomass produced in EBPR reactors to landfills. It can also be produced very economically on site, requiring a simple bioreactor or set of bioreactors, without the requirements of sterility or heating. Recovery of the actinide from the biomass could be performed via acidification to digest the biological material, followed by neutralization to a pH required for reprecipitation of uranyl phosphate. Noting that most of the precipitate tends to be on the outside of cells, recovery could be performed via a process that produces high shear,

such as a rapid bubbling or mixing. In this case, one would be required to differentially settle the precipitate from the biomass, which, depending on the size of biomass flocs, may or may not be a problem.

For the more general case of mixed metal waste streams, many other insoluble metal phosphates would precipitate. For that reason, one would expect to have little control over the order of precipitation of the metals in a mixed metal stream, which would be controlled by thermodynamics and the magnitudes of the specific solubility products in question. Furthermore, it may be necessary in certain situations to over-engineer the system such that enough phosphate is released to precipitate both secondary, less soluble metal phosphates and the metal phosphate(s)to be remediated.

This work represents one of the first studies concentrating on the use of organisms that perform a specific process to remove heavy metals and actinides rather than the isolation of organisms for their metal binding capabilities or the engineering of an organism to produce such an effect. This targeted approach has proven to be very effective, producing biomass with a possible uranyl-binding capacity nearly as high as any reported in the literature.

Acknowledgements

The authors would like to thank Andrew Magarosy and Chuch Echer for their assistance with the electron microscopy and EDXS. This work was funded by the NABIR program of the US Department of Energy.

References

Alonso A, Sanchez P et al. (2000) Stenotrophomonas maltophilia D457R contains a cluster of genes from gram-positive bacteria involved in antibiotic and heavy metal resistance. Antimicrobial Agents and Chemotherapy 44(7): 1778–1782

Ault-Riche D, Fraley CD et al. (1998) Novel assay reveals multiple pathways regulating stress-induced accumulations of inorganic polyphosphate in *E. coli*. J. Bacteriol. 180: 1841–1847

Bang SW, Clark DS et al. (2000) Engineering hydrogen sulfide production and cadmium removal by expression of the thiosulfate reductase gene *(phsABC)* from *Salmonella enterica* serovar Typhimurium in Escherichia coli. Appl. Environ. Microbiol. 66(9): 3939–3944

Bernhard G, Geipel G et al. (1996) Speciation of uranium in seepage waters of a mine tailing pile studied by time-resolved laser-induced fluorescence spectroscopy (TRLFS) Radiochimica Acta 74: 87–91

Chen S & Wilson DB (1997) Genetic engineering of bacteria and their potential for Hg^{2+} bioremediation. Biodegrad. 8(2): 97–103

Crocetti GR, Hugenholtz P et al. (2000) Identification of polyphosphate-accumulating organisms and design of 16S rRNA-directed probes for their detection and quantitation. Appl. Environ. Microbiol. 66(3): 1175–1182

Fredrickson JK, Kostandarithes HM et al. (2000) Reduction of Fe(III), Cr(VI), U(VI), and Tc(VII) by Deinococcus radiodurans R1. Appl. Environ. Microbiol. 66(5): 2006–2011

Fritz JS. & Bradford EC (1958) Detection of thorium and uranium. Analyt. Chem. 30: 1021–1022

Hesselmann RP, Werlen C et al. (1999) Enrichment, phylogenetic analysis and detection of a bacterium that performs enhanced biological phosphate removal in activated sludge. Systematic Appl. Microbiol. 22(3): 454–465

Kato Y, Meinrath G et al. (1994) A study of U(Vi) hydrolysis and carbonate complexation by time-resolved laser-induced fluorescence spectroscopy (TRLFS). Radiochimica Acta 64(2): 107–111

Keasling JD & Hupf GA (1996) Genetic manipulation of polyphosphate metabolism affects cadmium tolerance in *E. coli*. Appl. Environ. Microbiol. 62: 743–746

Kitamura A, Yamamura T et al. (1998) Measurement of hydrolysis species of U(VI) by time-resolved laser induced fluorescence spectroscopy. Radiochimica Acta 82: 147–152

Llanos J, Capasso C et al. (2000) Susceptibility to heavy metals and cadmium accumulation in aerobic and anaerobic thermophilic microorganisms isolated from deep-sea hydrothermal vents. Curr. Microbiol. 41(3): 201–205

Lovley DR (1995) Bioremediation of organic and metal contaminants with dissimilatory metal reduction. J. Indust. Microbiol. 14(2): 85–93

Macaskie LE (1990) An immobilized cell bioprocess for the removal of heavy metals from aqueous flows. J. Chem. Technol. Biotechnol. 49: 357–379

Macaskie LE & Dean ACR (1982) Cadmium removal by microorganisms. Environ. Technol. Lett. 3: 49–56

Macaskie LE, Dean ACR et al. (1992) Uranium bioaccumulation by a *Citrobacter* sp. as a result of enxymatically-mediated growth of polycristalline HUO_2PO_4. Science 257: 782–784

Macaskie LE, Dean ACR et al. (1987) Cadmium accumulation by a *Citrobacter* sp.: The chemical nature of the accumulated metal precipitate and its location on the bacterial cells. J. Gen. Microbiol. 133: 539–544

Mallick N, Shardendu et al. (1996) Removal of heavy metals by two free floating aquatic macrophytes. Biomed. Environ. Sci. 9(4): 399–407

Moulin C, Decambox P et al. (1994) Time-resolved laser-induced fluorescence of UO_2^{2+} in nitric acid solutions – comparison between nitrogen and tripled Nd-Yag laser. J. Nuclear Sci. Technol. 31(7): 691–699

Moulin C, Decambox P et al. (1995) Uranium speciation in solution by time-resolved laser-induced fluorescence. Analyt. Chem. 67(2): 348–353

Nies DH (2000) Heavy metal-resistant bacteria as extremophiles: Molecular physiology and biotechnological use of *Ralstonia* sp. CH34. Extremophiles 4(2): 77–82

Sharfstein ST, Van Dien SJ et al. (1996) Modulation of the phosphate-starvation response in *E. coli* by genetic manipulation of the polyphosphate pathways. Biotechnol. Bioengng. 51: 434–438

Sharma PK, Balkwill DL et al. (2000) A new *Klebsiella planticola* strain (Cd-1) grows anaerobically at high cadmium concentrations and precipitates cadmium sulfide. Appl. Environ. Microbiol. 66(7): 3083–3087

Smolders GJF, Van der Meij J et al. (1994) Model of the anaerobic metabolism of the biological phosphorus removal process: Stoichiometry and pH influence. Biotechnol. Bioengng. 43(6): 461–470

Travieso L, Cañizares RO et al. (1999) Heavy metal removal by microalgae. Bull. Environ. Contamin. Toxicol. 62(2): 144–151

Tucker MD, Barton LL et al. (1998) Reduction of Cr, Mo, Se and U by Desulfovibrio desulfuricans immobilized in polyacrylamide gels. *Journal of Industrial Microbiol. Biotechnol.* 20(1): 13–19

Valls M, de Lorenzo V et al. (2000) Engineering outer-membrane proteins in *Pseudomonas putida* for enhanced heavy-metal bioadsorption. J. Inorg. Biochem. 79(1–4): 219–223.

Van Loosdrecht MCM, Hooijmans CM et al. (1997) Biological phosphate removal processes. Appl. Microbiol. Biotechnol. 48: 289–296.

Van Veen HW, Abee T et al. (1994) Generation of a proton motive force by the excretion of metal-phosphate in the polyphosphate-accumulating *Acinetobacter johnsonii* strain 210A. J. Biologic. Chem. 269(47): 29509–29514

Volesky B (1990) Biosorption of heavy metals. CRC Press, Boca Raton, FL.

Wang CL, Maratukulam PD et al. (2000) Metabolic engineering of an aerobic sulfate reduction pathway and its application to precipitation of cadmium on the cell surface. Appl. Environ. Microbiol. 66(10): 4497–4502

Wang CL, Michels PC et al. (1997) Cadmium removal by a new strain of *Pseudomonas aeruginosa* in aerobic culture. Appl. Environ. Microbiol. 63(10): 4075–4078

Wang TC, Weissman JC et al. (1998) Heavy metal binding and removal by phormidium. *Bulletin of Environmental Contamination and Toxicology* 60(5): 739–744

Wentzel MC, Loewenthal RE et al. (1988) Enhanced polyphosphate organism cultures in activated sludge systems: Part 1: Enhanced culture development. Water S A (Pretoria) 14(2): 81–92

Xiang L, Chan LC et al. (2000) Removal of heavy metals from anaerobically digested sewage sludge by isolated indigenous iron-oxidizing bacteria. Chemosphere 41(1–2): 283–287

Yong P. & Macaskie LE (1995) Role of citrate as a complexing ligand which permits enzymically-mediated uranyl ion bioaccumulation. Bull. Environ. Contamin. Toxicol. 54: 892–899.